Eur J Appl Physiol (2013) 113:591–598
DOI 10.1007/s00421-012-2469-7

ORIGINAL ARTICLE

Influence of end-expiratory level and tidal volume on gravitational ventilation distribution during tidal breathing in healthy adults

Silvia Schnidrig · Carmen Casaulta · Andreas Schibler · Thomas Riedel

Received: 9 February 2012 / Accepted: 25 July 2012 / Published online: 8 August 2012

Abstract Our understanding of regional filling of the lung and regional ventilation distribution is based on studies using stepwise inhalation of radiolabelled tracer gases, magnetic resonance imaging and positron emission tomography. We aimed to investigate whether these differences in ventilation distribution at different end-expiratory levels (EELs) and tidal volumes (V_Ts) held also true during tidal breathing. Electrical impedance tomography (EIT) measurements were performed in ten healthy adults in the right lateral position. Five different EELs with four different V_Ts at each EEL were tested in random order, resulting in 19 combinations. There were no measurements for the combination of the highest EEL/highest V_T. EEL and V_T were controlled by visual feedback based on airflow. The fraction of ventilation directed to different slices of the lung ($VENT_{RL1}-VENT_{RL8}$) and the rate of the regional filling of each slice versus the total lung were analysed. With increasing EEL but normal tidal volume, ventilation was preferentially distributed to the dependent lung and the filling of the right and left lung was more homogeneous. With increasing V_T and maintained normal EEL (FRC), ventilation was preferentially distributed to the dependent lung and regional filling became more inhomogeneous ($p < 0.05$). We could demonstrate that regional and temporal ventilation distribution during tidal breathing was highly influenced by EEL and V_T.

Keywords Lung mechanics · Electrical impedance tomography · Regional filling · Breathing pattern

Introduction

Over the last few decades, several studies have described ventilation distribution (VD) of the healthy lung and have found that gravity, size of the tidal volume, inspiratory flow rate and end-expiratory level impact on regional VD and specific ventilation (SV) (Fixley et al. 1978; Grant et al. 1974a, b; Kaneko et al. 1966; Milic-Emili et al. 1966; Robertson et al. 1969; Roussos et al. 1977; West 1966). VD and SV can be measured using either multiple breath inert tracer gas washout techniques with radiolabelled tracer gases combined with imaging, or recently with PET, hyperpolarized helium and oxygen-enhanced proton MRI (Emami et al. 2010; Musch et al. 2002; Robinson et al. 2009; Sa et al. 2010; West 1966). Inert gas washout techniques can measure global VD, but cannot differentiate between regional ventilation differences (Robinson et al. 2009).

Imaging techniques can identify regional differences, but have a low temporal resolution. Because of the slow sampling rate, the impact of the respiratory pattern cannot be directly assessed, but rather only estimated from stepwise inspirations with breath-hold techniques or the measurement of a single tidal breath (Grant et al. 1974b; Milic-Emili et al.

Communicated by Susan A. Ward.

S. Schnidrig · T. Riedel (✉)
Division of Paediatric and Neonatal Intensive Care Medicine, Department of Paediatrics, Inselspital, University Children's Hospital and University of Bern, 3010 Bern, Switzerland
e-mail: thomas.riedel@insel.ch

C. Casaulta
Division of Paediatric Respiratory Medicine, Department of Paediatrics, Inselspital, University Children's Hospital and University of Bern, Bern, Switzerland

A. Schibler · T. Riedel
Paediatric Critical Care Research Group, Paediatric Intensive Care Unit, Mater Children's Hospital, South Brisbane, QLD, Australia

1966). In this way, information on a dynamic process is generated by interpolating sequences of static measures.

Electrical impedance tomography (EIT) can measure relative changes in end-expiratory level (EEL) and regional differences in VD and does not interfere with the breathing pattern (Dunlop et al. 2006; Frerichs 2000; Grant et al. 2009; Pham et al. 2010; Riedel et al. 2005, 2009; Rooney et al. 2009). While EIT only measure EEL and VD of the cross-sectional area where the electrodes are applied, it can still be used to quantify the relative impact of different breathing patterns on regional VD.

Our understanding of regional filling of the lung and regional VD is based on the above-mentioned studies using stepwise inhalation with radiolabelled tracer gases. In this study, we investigated whether the same regional filling characteristics and regional VD can be demonstrated during tidal breathing in healthy adults. In order to maximize the impact of gravity on VD, measurements were performed in the lateral position.

Methods

Study design

The study was approved by the local ethics committee and performed at the University Children's Hospital Bern, Switzerland, between October and November 2010. Electrical impedance tomography (EIT) measurements were performed in ten healthy, non-smoking adults (6 femalea) aged 29–50 years, weight 53–93 kg in the *right lateral* body position (left lung uppermost). In total, 19 different combinations of end-expiratory level (EEL) and tidal volume (V_T) were tested in each participant in random order. EEL and V_T were controlled by the subject using visual feedback.

Investigated breathing patterns

Five EELs were investigated: increases and decreases of 0.5 and 1.0 normal V_T from normal resting EEL (EEL $-$ $\Delta 1V_T$, EEL $-$ $\Delta 0.5V_T$, EEL, EEL $+$ $\Delta 0.5V_T$ and EEL $+$ $\Delta 1V_T$). At each of these five different EELs, proportional changes in V_Ts were assessed: $0.5V_T$, $1V_T$, $1.5V_T$, and $2V_T$. There were no measurements for the combination of EEL $+$ $\Delta 1V_T$ with $2V_T$, as it was not possible for most of the individuals to achieve this breathing pattern. Hence, there were in total 19 breathing combinations that were performed in a random order for each subject investigated.

Data acquisition and bio-feedback

EIT measurements were performed using the Goettingen EIT GoeMFII (CareFusion, The Netherlands) with a frame rate of 13 Hz and a 30 s recording time in combination with Ambu® Blue Sensor T self-adhesive electrodes (Synmedic, Switzerland) equally distributed around the chest at the xyphoid level. To allow the investigated subject to maintain a changed EEL and different sizes of V_T, the EEL and volume trace, recorded with a ultrasonic flow meter (Spiroson Scientific, Ecomedics, Switzerland), were visualized on the screen of a laptop computer with the software provided by the manufacturer (Spiroware© 2.0). A low resistance bacterial filter (Hygrovent S, Medisize, The Netherlands) was placed between the subject and the flow head resulting in a technical dead space of 8.5 ml. A nose clip was used throughout the measurements. For each measurement, the subject was breathing initially at normal EEL with normal V_T. After a stable period, the subject was instructed to change the EEL to the required level and adapt the V_T. Once the required EEL and V_T was achieved, an EIT measurement of 30 s was recorded. V_T at the mouth, measured with an ultrasonic flow meter, was recorded for each breathing pattern combination. Mean V_T over 30 s was used for further analysis. The change in EEL measured with EIT was expressed in normalized V_T units, i.e., a change in EEL by 1 was equivalent to a change by a mean normal V_T at normal EEL. This method allowed a comparison of the change in EEL measured by the flow meter and EIT.

Data analysis

EIT scans were generated using weighted back-projection with software provided by the manufacturer in a 32 × 32 pixel matrix. The EIT signal was low-pass filtered below the cardiac frequency and a cutoff mask of 20 % of the maximum standard deviation was used (Dunlop et al. 2006; Pulletz et al. 2006). The values were averaged over a cross-sectional EIT slice, whereby the exact thickness of this slice could not be precisely determined. In an adult, it is estimated to be approximately 7–10 cm (Costa et al. 2009).The fraction of ventilation distributed into eight different slices of the lung ($VENT_{RL1–8}$, with $VENT_{RL1}$ being the most dependent and $VENT_{RL8}$ being the most non-dependent slice) (Fig. 1), end-expiratory level (EEL) and regional filling characteristics of each slice were calculated as previously described using custom software programmed in Matlab 7.1 (The Mathworks Inc., Nattick, MA, USA) (Riedel et al. 2005). The fraction of the ventilation distributed into the different slices, $VENT_{RL1–8}$, was calculated by dividing the EIT image into eight slices from right to left, and calculating the proportion of each slice contributing to the total impedance change. For the calculation of the regional filling characteristics, the impedance change of each slice was plotted against the global impedance change for each recorded breath. The resulting

curve was fitted to the following equation using a Levenberg–Marquardt method:

$$I(g) = a \times g^{FI} + c$$

where *I(g)* is the impedance change of the respective slice, g is the impedance change of the global signal, and the filling index (FI) describes the shape of the curve(Grant et al. 2009). If FI > 1, the rate of volume change in the respective slice is lower than the rest of the lung during the initial phase of inspiration, but increases towards the end of inspiration. In contrast, if FI < 1, the rate of volume change in the respective slice is greater during the initial phase of the inspiration, but decreases towards the end of inspiration.

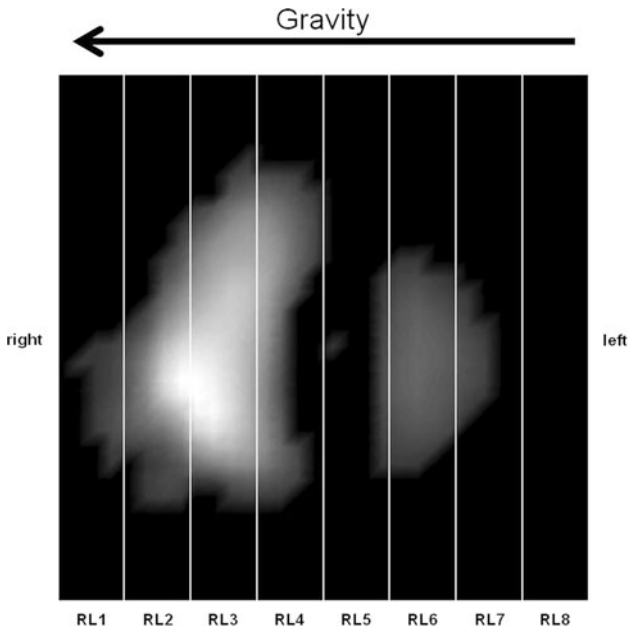

Fig. 1 Example of an EIT image at FRC + 0.5 and normal V_T showing RL1–8

Statistics

Data are presented with mean and 95 % confidence intervals (CI). For differences in regional ventilation distribution at different EELs and V_Ts, a Friedman test with correction for multiple comparisons was used. A p value < 0.05 was considered to be significant. All statistics were performed using StatsDirect®, version 2.7.7 (StatsDirect Ltd., GB).

Results

V_T measured with the flow meter during regular breathing ranged between 420 and 720 ml, equivalent to 7–9 ml/kg body weight. There was a difference between the target V_T and measured V_T for most of the breathing combinations. Measured V_T differed from target V_T (0.5, 1.5 and 2 × normal) by −6 (−11 to −1) % at 2 × normal V_T to 8 (3–13) % at 0.5 × normal V_T. (Table 1) Effective EEL measured by EIT was slightly lower at target EEL (visual feedback) below normal FRC, and at target above normal FRC (Table 2).

Impact of change of EEL on VD during regular tidal breathing (Fig. 2)

This analysis was only performed for slices RL2–RL7 because most of the subjects showed no ventilation in slices RL1 and RL8, suggesting there was no lung in these areas. In the right lateral position during regular breathing at the lowest investigated EEL (EEL − $\Delta 1V_T$), ventilation was preferentially distributed to the left (independent) parts of the lung ($p < 0.01$). An increase in EEL by steps of $\Delta 0.5V_T$ up to EEL + $\Delta 1V_T$ continuously increased the proportion of ventilation distributed to the right (dependent) parts of the lungs. This change was statistically significant in all slices from RL2 to RL7 ($p < 0.01$ for all slices).

Table 1 Target V_T calculated from spontaneous V_T at normal FRC and V_T achieved by visual feedback measured by ultrasonic flow meter

	$0.5V_T$ (ml)	$1.5V_T$ (ml)	$2V_T$ (ml)
Target V_T	265 (226–304)	797 (680–914)	1,060 (904–1214)
Target V_T/kg	4 (3.8–4.2)	12 (11.5–12.5)	16 (15.3–16.7)
Achieved V_T	285 (243–327)	790 (674–906)	1,002 (854–1,150)
Achieved V_T/kg	4.3 (4.1–4.5)	11.9 (11.4–12.4)	15.0 (14.2–15.8)

Results are given as mean (95 %CI)

Table 2 Target EEL and achieved EEL measured by EIT (EEL_{EIT})

	EEL − $\Delta 1V_T$	EEL − $\Delta 0.5V_T$	EEL + $\Delta 0.5V_T$	EEL + ΔV_T
EEL_{EIT}	−0.76 (−0.67 to −0.85)	−0.41 (−0.32 to −0.50)	0.48 (0.36–0.60)	0.94 (0.72–1.16)

Values are expressed as difference to normal FRC normalized to spontaneous V_T at normal FRC. Results are given as mean (95 %CI)

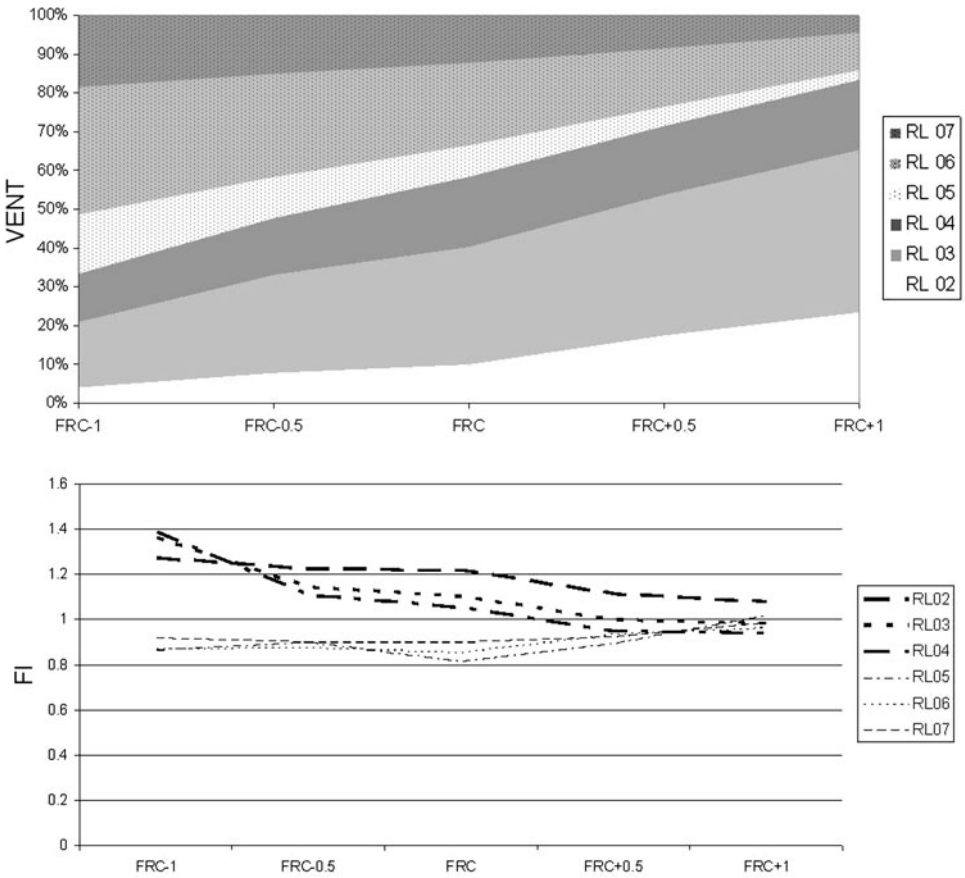

Fig. 2 Spatial (*upper panel*) and temporal (*lower panel*) ventilation distribution in relation to EEL breathing at normal V_T. *VENT* proportion of ventilation distributed to the respective slice, *FI* filling index for the respective slice in relation to the total lung. For clarity of the figure, no significance levels are indicated

The regional filling characteristics during regular breathing were also dependent on the EEL. The lower the EEL, the slower was the filling of the right parts of the lung during the initial phase of inspiration. With increasing EEL, the temporal filling of both the left and right lung became more even. This change was statistically significant in slices RL2–4 and slice RL7 ($p < 0.01$).

Impact of different sized V_T on VD at normal EEL (FRC) (Fig. 3)

Again, this analysis was only performed for slices RL2–RL7 because most of the subjects showed no ventilation in slices RL1 and RL8. Ventilation was evenly distributed between the right (dependent) and left (independent) lung at normal EEL with half of the normal tidal volume. With increasing V_T from 0.5 to 2 × normal V_T, the proportion of ventilation increased significantly ($p < 0.01$) in slices RL2–RL4 and decreased significantly ($p < 0.01$) in slices RL5–RL7. Similarly, the filling characteristics showed a trend towards increasing FI of the right lung with increasing V_T, which was only statistically significant for slice RL2 ($p < 0.05$) and significantly faster filling of all the slices of the left lung ($p < 0.01$ for slices RL5–7).

Impact of different sized V_T in combination with different EEL on VD (Fig. 4)

To simplify these complex results, only the proportion of ventilation distributed to the right lung $VENT_{right}$ (combination of slices RL1–4) is shown. The greatest impact of the size of V_T on VD was demonstrated when EEL was below normal FRC. With increasing EEL, the impact of the size of V_T was less obvious. Figure 4 demonstrates that both, EEL and size of V_T, determine ventilation distribution.

Discussion

We could demonstrate that regional and temporal ventilation distribution during tidal breathing is highly dependent on EEL and V_T. The effects can be summarized as follows: with increasing EEL but normal tidal breathing, ventilation was preferentially distributed to the dependent lung and the filling characteristics were more homogeneous. With increasing V_T and maintained normal EEL, ventilation was preferentially distributed to the dependent lung and regional filling became more inhomogeneous. Our findings during tidal breathing are in line with the results of

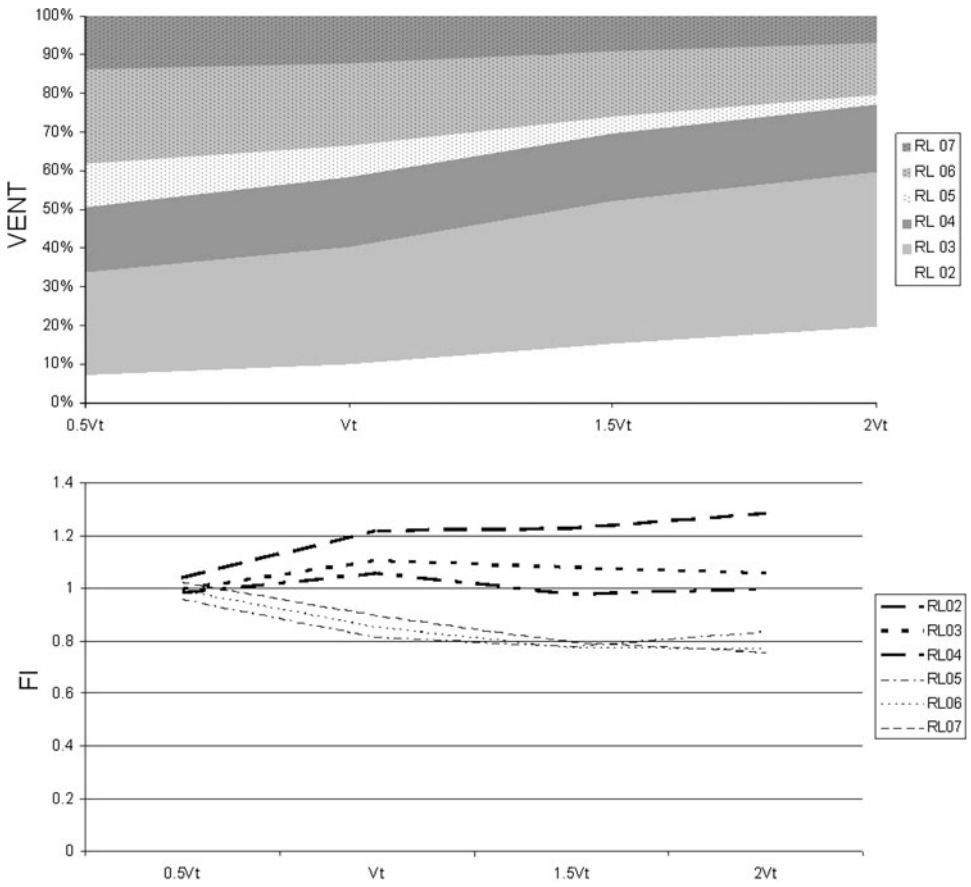

Fig. 3 Spatial (*upper panel*) and temporal (*lower panel*) ventilation distribution in relation to V_T breathing at normal EEL. *VENT* proportion of ventilation distributed to the respective slice, *FI* filling index for respective slice in relation to the total lung. For clarity of the figure, no significance levels are indicated

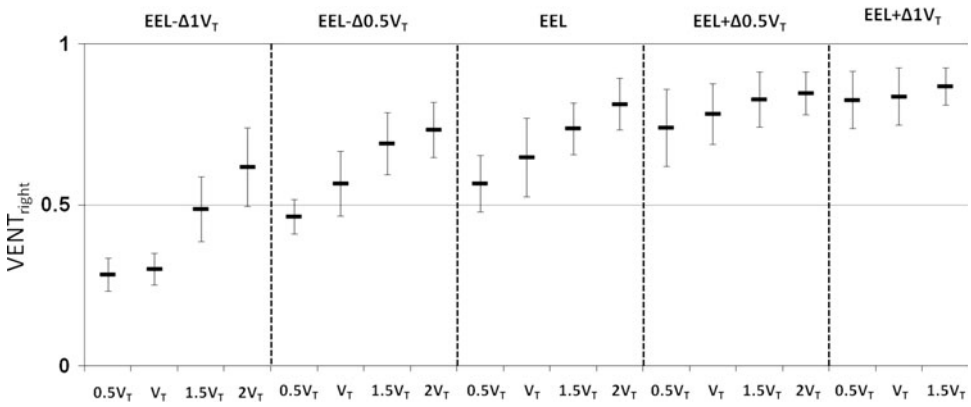

Fig. 4 Spatial ventilation distribution in relation to different combinations of V_T and EEL. $VENT_{right}$: proportion of ventilation distributed to the right (dependent) parts of the lung. For clarity of the figure, no significance levels are indicated

previous studies using stepwise inflation manoeuvres (Grant et al. 1974b; Kaneko et al. 1966; Milic-Emili et al. 1966).

Impact of change of EEL and V_T on VD during regular breathing

Milic-Emili and co-workers published a study evaluating the influence of EEL and V_T on the distribution of gas within the lung. They used a gas-dilution technique with Xe^{133} and stepwise inspirations of different tidal volumes from different EELs, expressed as percentage of the total lung capacity (TLC) or percentage of vital capacity (VC). They found that static regional volumes were always greater in the upper than lower lung zones. Further, it could be shown that changes in regional volumes (ventilation) were greater in the upper zones of the lung when EEL was low (≤20 % VC), and ventilation was greater in the lower zones of the lung when EEL was high (Milic-Emili et al. 1966). These results could also be confirmed in different body positions by the same group (Kaneko et al. 1966). Our study demonstrated that these findings held also true

during tidal breathing with the non-dependent lung being preferentially ventilated when EEL was low and the dependent lung better ventilated at high EEL (Fig. 2). Using the Xe^{133} inhalation imaging technique, the rate of regional volume change in the apical lung was greater than the volume change of the global lung during the initial phase of inspiration, but was curvilinear once the apical lung volume was >20 % of the regional vital capacity (VCr). The rate of volume change in the lower lung during the initial phase of inspiration was smaller than the volume change of the global lung, but was again curvilinear once the lower lung volume was >20 % of the regional VCr (Kaneko et al. 1966; Milic-Emili et al. 1966). Our measurements using EIT are in agreement with these gravity-dependent differences in regional VD and demonstrated that the regional expansion was not uniform, with the dependent lung (the right lung in our experiment) expanding with a lower rate than the non-dependent lung during the initial phase of inspiration, but with a higher rate towards the end of inspiration even during tidal breathing. In contrast to the Xe^{133} inhalation imaging technique, EIT allows a continuous measurement of the filling characteristics of the lung during tidal breathing (Grant et al. 2009). This advantage of the EIT measurement technique has already been used in clinical studies investigating lung recruitment in ventilated patients (Tingay et al. 2010; Wrigge et al. 2008).

As mentioned earlier, ventilation is preferentially distributed to the upper lung zones only at EEL close to the residual volume (RV). Additionally, we could show that this holds only true with small to normal V_T and the effect can be overcome by increasing V_T (Fig. 4). The most likely explanation for this fact was that EEL decreased below the closing volume of the dependent parts of the lung. By increasing V_T, we could achieve tidal recruitment of the right lung and therefore a more even spatial distribution as shown with $1.5V_T$ and $2V_T$. The effect of increasing tidal volume on spatial distribution diminishes with increasing EEL and gets lost at the highest EEL (EEL + $\Delta 1V_T$). This can be explained by an increasing over-inflation of the right lung leading to more homogenous temporal filling as shown in Fig. 2.

In addition to the results of Milic-Emili at al. and Kaneko et al., we found a curvilinear relationship between the change in regional and total lung volume up to an EEL of normal FRC with normal and high V_T and even above normal FRC with high V_T, highlighting the effect of tidal volume. The FI > 1 of slices RL2–4 indicates slow early filling of the right (dependent) lung. These results are supported by another study where sequential portions of the inspired gas were labelled with Xe^{133}. During normal tidal breathing, the gas in the trachea and upper airways (early) was distributed preferentially to the upper zones of the lungs on inspiration, whereas the gas from the mouth and from added dead space (late) was preferentially distributed to the lower zones of the lung (Grant et al. 1974b).

Because of the nature of EIT (cross-sectional image of the chest), our experiments were all performed in the right lateral position, unlike most of the studies using Xe133-labelled gas which were performed in an upright position; but gravity-dependent ventilation distribution seemed to be similar in both upright and right lateral positions (Rehder et al. 1977). Nevertheless, we cannot rule out that the different findings compared to the work of Milic-Emili could be caused by different body positions. EIT has been used to determine ventilation distribution in different body positions in several studies showing distinct differences between preterm and term babies and between young and elderly adults (Frerichs et al. 1996, 2001, 2004; Pham et al. 2010; Riedel et al. 2005, 2009 Schibler et al. 2009). In young healthy adults with passive elevation of EEL under continuous positive airway pressure (CPAP), we found similar results compared to the present study with active elevation of EEL where spatial distribution towards the upper lung zones is increased (Riedel et al. 2005). These similarities between active and passive elevation of EEL suggest that the change in spatial ventilation distribution with higher EEL is not caused by differences in muscle activity, but the increase of EEL itself.

In the present study, we did not examine the influence of different flow rates on ventilation distribution. Grant et al. (1974b) showed inspiratory flow dependency mainly of the first portions of V_T, whereas the last portions showed similar behaviour at all tested flow rates. In a group of four young healthy adults performing vital capacity manoeuvres at different flow rates (0.3–1.3 l/s), we could demonstrate more even temporal ventilation distribution only with the highest inspiratory flow of 1.3 l/s, whereas spatial distribution showed a continuous shift towards more homogeneous distribution with increasing flow rates (unpublished data). Based on these results, the effect of inspiratory flow rates during tidal breathing at different EEL and V_T should be negligible.

To our knowledge, this is the first study investigating the influence of EEL and V_T on ventilation distribution during spontaneous tidal breathing in adults. We could achieve distinct and reproducible breathing patterns with respect to EEL and V_T by simple visual biofeedback. Nevertheless, the study has some limitations. First, all measurements were performed in the right lateral position. We decided to do so because gravitational effects on ventilation distribution seem to be greatest in this position and because EIT, by its nature of measurements, is unable to detect differences in ventilation in a sagittal or frontal plane. Despite this, we could show similar results compared to the studies performed in an upright position, showing that changes

along the gravitational axis are consistent in upright and right lateral positions. Systems allowing simultaneous measurements of different planes might be able to overcome this problem in the future. Second, EIT analysis is not linked to any fixed anatomical point, leading to the fact that different parts of the lung will be analysed with different EEL and V_T. By averaging data over the whole thickness of the analysed cross-sectional slices (several centimetres), the impact of this potential downside should be minimal and might even improve the robustness of our results by increasing the accuracy of differences found in the gravity axis. Future development of better EIT systems might increase resolution and allow a refined analysis. Additionally, despite using multiple slices of the lung, spatial resolution is still low compared to other techniques, such as computer tomography, MRI or PET (Costa et al. 2009). We analysed more different regions than most of the studies investigating ventilation distribution in the past (Grant et al. 2009; Hahn et al. 1995; Heinrich et al. 2006; Pham et al. 2010; Riedel et al. 2005, 2009; Schibler et al. 2009). The volume/voxel and therefore the thickness of a slice RL_1–RL_8 is dependent on the chest diameter and cannot be expressed in ml and cm, respectively. This potential limitation of EIT might even be an advantage in our study because comparison of different sized adults can easily be performed.

In conclusion, electrical impedance tomography is able to characterize the influence of end-expiratory level and tidal volume on spatial and temporal ventilation distribution during spontaneous tidal breathing.

Conflict of interest No conflicts of interest, financial or otherwise, are declared by the authors.

References

Costa EL, Lima RG, Amato MB (2009) Electrical impedance tomography. Curr Opin Crit Care 15:18–24

Dunlop S, Hough J, Riedel T, Fraser JF, Dunster K, Schibler A (2006) Electrical impedance tomography in extremely prematurely born infants and during high frequency oscillatory ventilation analyzed in the frequency domain. Physiol Meas 27:1151–1165

Emami K, Kadlecek SJ, Woodburn JM, Zhu J, Yu J, Vahdat V, Pickup S, Ishii M, Rizi RR (2010) Improved technique for measurement of regional fractional ventilation by hyperpolarized 3He MRI. Magn Reson Med 63:137–150

Fixley MS, Roussos CS, Murphy B, Martin RR, Engel LA (1978) Flow dependence of gas distribution and the pattern of inspiratory muscle contraction. J Appl Physiol 45:733–741

Frerichs I (2000) Electrical impedance tomography (EIT) in applications related to lung and ventilation: a review of experimental and clinical activities. Physiol Meas 21:R1–R21

Frerichs I, Hahn G, Hellige G (1996) Gravity-dependent phenomena in lung ventilation determined by functional EIT. Physiol Meas 17 Suppl 4A:A149–157

Frerichs I, Dudykevych T, Hinz J, Bodenstein M, Hahn G, Hellige G (2001) Gravity effects on regional lung ventilation determined by functional EIT during parabolic flights. J Appl Physiol 91:39–50

Frerichs I, Braun P, Dudykevych T, Hahn G, Genee D, Hellige G (2004) Distribution of ventilation in young and elderly adults determined by electrical impedance tomography. Respir Physiol Neurobiol 143:63–75

Grant BJ, Jones H, Hughes JM (1974a) Inspiratory flow rate and ventilation distribution. Scand J Respir Dis Suppl 85:23–27

Grant BJ, Jones HA, Hughes JM (1974b) Sequence of regional filling during a tidal breath in man. J Appl Physiol 37:158–165

Grant CA, Fraser JF, Dunster KR, Schibler A (2009) The assessment of regional lung mechanics with electrical impedance tomography: a pilot study during recruitment manoeuvres. Intensive Care Med 35:166–170

Hahn G, Sipinkova I, Baisch F, Hellige G (1995) Changes in the thoracic impedance distribution under different ventilatory conditions. Physiol Meas 16:A161–A173

Heinrich S, Schiffmann H, Frerichs A, Klockgether-Radke A, Frerichs I (2006) Body and head position effects on regional lung ventilation in infants: an electrical impedance tomography study. Intensive Care Med 32:1392–1398

Kaneko K, Milic-Emili J, Dolovich MB, Dawson A, Bates DV (1966) Regional distribution of ventilation and perfusion as a function of body position. J Appl Physiol 21:767–777

Milic-Emili J, Henderson JA, Dolovich MB, Trop D, Kaneko K (1966) Regional distribution of inspired gas in the lung. J Appl Physiol 21:749–759

Musch G, Layfield JD, Harris RS, Melo MF, Winkler T, Callahan RJ, Fischman AJ, Venegas JG (2002) Topographical distribution of pulmonary perfusion and ventilation, assessed by PET in supine and prone humans. J Appl Physiol 93:1841–1851

Pham TM, Yuill M, Dakin C, Schibler A (2010) Regional ventilation distribution in the first 6 months of life. Eur Respir J

Pulletz S, van Genderingen HR, Schmitz G, Zick G, Schadler D, Scholz J, Weiler N, Frerichs I (2006) Comparison of different methods to define regions of interest for evaluation of regional lung ventilation by EIT. Physiol Meas 27:S115–S127

Rehder K, Sessler AD, Rodarte JR (1977) Regional intrapulmonary gas distribution in awake and anesthetized-paralyzed man. J Appl Physiol 42:391–402

Riedel T, Richards T, Schibler A (2005) The value of electrical impedance tomography in assessing the effect of body position and positive airway pressures on regional lung ventilation in spontaneously breathing subjects. Intensive Care Med 31:1522–1528

Riedel T, Kyburz M, Latzin P, Thamrin C, Frey U (2009) Regional and overall ventilation inhomogeneities in preterm and term-born infants. Intensive Care Med 35:144–151

Robertson PC, Anthonisen NR, Ross D (1969) Effect of inspiratory flow rate on regional distribution of inspired gas. J Appl Physiol 26:438–443

Robinson PD, Goldman MD, Gustafsson PM (2009) Inert gas washout: theoretical background and clinical utility in respiratory disease. Respiration 78:339–355

Rooney D, Friese M, Fraser JF, Dunster KR, Schibler A (2009) Gravity-dependent ventilation distribution in rats measured with electrical impedance tomography. Physiol Meas 30:1075–1085

Roussos CS, Fixley M, Genest J, Cosio M, Kelly S, Martin RR, Engel LA (1977) Voluntary factors influencing the distribution of inspired gas. Am Rev Respir Dis 116:457–467

Sa RC, Cronin MV, Henderson AC, Holverda S, Theilmann RJ, Arai TJ, Dubowitz DJ, Hopkins SR, Buxton RB, Prisk GK (2010) Vertical distribution of specific ventilation in normal supine humans measured by oxygen-enhanced proton MRI. J Appl Physiol 109:1950–1959

Schibler A, Yuill M, Parsley C, Pham T, Gilshenan K, Dakin C (2009) Regional ventilation distribution in non-sedated

spontaneously breathing newborns and adults is not different. Pediatr Pulmonol 44:851–858

Tingay DG, Copnell B, Grant CA, Dargaville PA, Dunster KR, Schibler A (2010) The effect of endotracheal suction on regional tidal ventilation and end-expiratory lung volume. Intensive Care Med 36:888–896

West JB (1966) Distribution of pulmonary blood flow and ventilation measured with radioactive gases. Scand J Respir Dis Suppl 62:9–13

Wrigge H, Zinserling J, Muders T, Varelmann D, Gunther U, von der Groeben C, Magnusson A, Hedenstierna G, Putensen C (2008) Electrical impedance tomography compared with thoracic computed tomography during a slow inflation maneuver in experimental models of lung injury. Crit Care Med 36:903–909